

# Supplementary Material to:

## Parallax Bundle Adjustment on Manifold with Improved Global Initialization

Liyang Liu, Teng Zhang, Yi Liu, Brenton Leighton, Liang Zhao, Shoudong Huang, and Gamini Dissanayake

University of Technology Sydney, Sydney NSW 2007, Australia

This report provides theorem proofs, additional derivations and experimental results to support the paper [1]. Therefore, it should not be considered a self-contained document, but rather regarded as an appendix of [1], and cited as:

*“L. Liu, T. Zhang, Y. Liu, B. Leighton, L. Zhao, S. Huang, and G. Dissanayake, Parallax bundle adjustment on manifold with improved global initialization, (supplementary material)”*

## 1 The Proof of Theorem 1

**Theorem 1.** Under the formulation [1](9),  $\mathbf{H}_{\mathbf{FF}}$  is consistently non-singular for any  $\mathcal{X}$  and  $\mathbf{H}_{\mathbf{FF}} \geq \mathbf{I}$ .

Consider the feature  $j$  and the corresponding sub-block matrix  $\mathbf{H}_{\mathbf{FF}_j}$  in  $\mathbf{H}_{\mathbf{FF}} = blkdiag(\mathbf{H}_{\mathbf{FF}_1}, \dots, \mathbf{H}_{\mathbf{FF}_n})$ . Denote  $\mathbf{J}_{i,j} = \frac{\partial \mathbf{e}_{i,j}}{\partial \mathbf{F}_j}$  for  $(i \in \mathbb{T}_j)$ ,  $\mathbf{J}_{m_j,j}$  is the jacobian for the feature's main anchor observation,  $\mathbf{J}_{a_j,j}$  is the jacobian for its associate anchor observation. We have

$$\mathbf{H}_{\mathbf{FF}_j} \geq \mathbf{J}_{m_j,j}^\top \mathbf{J}_{m_j,j} + \mathbf{J}_{a_j,j}^\top \mathbf{J}_{a_j,j}. \quad (1)$$

On the one hand, using (28) in Appendix B , we have

$$\mathbf{J}_{m_j,j}^\top \mathbf{J}_{m_j,j} = \begin{bmatrix} \mathbf{0} & \mathbf{0} \\ \mathbf{0} & (S(\mathbf{n}_j)\mathbf{A}_{\mathbf{n}_j})^\top (S(\mathbf{n}_j)\mathbf{A}_{\mathbf{n}_j}) \end{bmatrix} = \begin{bmatrix} \mathbf{0} & \mathbf{0} \\ \mathbf{0} & \mathbf{I}_2 \end{bmatrix}. \quad (2)$$

On the other hand, we have

$$\mathbf{J}_{a_j,j}^\top \mathbf{J}_{a_j,j} \geq \left[ \frac{\partial \mathbf{e}_{i,j}}{\partial \theta_j} \mathbf{0} \right]^\top \left[ \frac{\partial \mathbf{e}_{i,j}}{\partial \theta_j} \mathbf{0} \right] = \begin{bmatrix} (\partial \xi \mathbf{J}_\theta^N)^\top (\partial \xi \mathbf{J}_\theta^N) & \mathbf{0} \\ \mathbf{0} & \mathbf{0} \end{bmatrix}, \quad (3)$$

where  $\partial \xi$  is the jacobian of normalize function with respect to ray  $\mathbf{N}_{a_j,j}$ , and  $\mathbf{J}_\theta^N$  is the jacobian of  $\mathbf{N}_{a_j,j}$  with respect to parallax angle  $\theta_j$ .

Using equation (29) from Appendix B

$$\mathbf{N}_{a_j,j} = \cos \theta_j \|\mathbf{a} \times \mathbf{n}_m\| \mathbf{n}_m + \sin \theta_j (\mathbf{a} - (\mathbf{a} \cdot \mathbf{n}_m) \mathbf{n}_m). \quad (4)$$

$$\mathbf{J}_\theta^N = -\sin(\theta) \|\mathbf{a} \times \mathbf{n}_m\| \mathbf{n}_m + \cos(\theta) (\mathbf{a} - (\mathbf{a}^\top \mathbf{n}_m) \mathbf{n}_m) \quad (5)$$

where

$$\mathbf{a} = \mathbf{p}_{m_j} - \mathbf{p}_{a_j}, \quad \mathbf{b} = \mathbf{p}_{m_j} - \mathbf{p}_i, \quad \mathbf{n}_m = \mathbf{R}_{m_j} \mathbf{n}_{m_j}.$$

Observe that

$$\begin{aligned} & (\mathbf{a} - (\mathbf{a} \cdot \mathbf{n}_m) \mathbf{n}_m) \perp \mathbf{n}_m, \\ & \|(\mathbf{a} - (\mathbf{a} \cdot \mathbf{n}_m) \mathbf{n}_m)\| = \|\mathbf{a} \times \mathbf{n}_m\| = \sin(\pi - \alpha_j), \end{aligned}$$

we have

$$\begin{aligned} \mathbf{N}_{a,j} \cdot \mathbf{J}_\theta^N &= 0 \\ \|\mathbf{N}_{a,j}\| &= \|\mathbf{J}_\theta^N\| = \lambda. \end{aligned}$$

Thus rewrite (4) as

$$\begin{aligned} \mathbf{N}_{a,j} &= \lambda \mathbf{u}, \quad \mathbf{u}^\top \mathbf{u} = 1 \\ \mathbf{J}_\theta^N &= \lambda \mathbf{v}, \quad \mathbf{v}^\top \mathbf{v} = 1 \\ \mathbf{u} \cdot \mathbf{v} &= 0. \end{aligned} \tag{6}$$

Substitute into (3) with the expression for normalize function's jacobian  $\partial \xi$  from Appendix B (18), we get

$$\partial \xi \mathbf{J}_\theta^N = (\mathbf{I}_3 - \mathbf{u} \mathbf{u}^\top) \mathbf{v} = \mathbf{v}. \tag{7}$$

Now we have

$$\begin{bmatrix} (\partial \xi \mathbf{J}_\theta^N)^\top (\partial \xi \mathbf{J}_\theta^N) & \mathbf{0} \\ \mathbf{0} & \mathbf{0} \end{bmatrix} = \begin{bmatrix} 1 & \mathbf{0} \\ \mathbf{0} & \mathbf{0} \end{bmatrix}. \tag{8}$$

Therefore,  $\mathbf{H}_{\mathbf{FF}_j} \geq \mathbf{I}_3$  and  $\mathbf{H}_{\mathbf{FF}} \geq \mathbf{I}$ .

## 2 Proof of Theorem 2

**Theorem 2.** *With accurate initial estimate for orientation, the formulation [1](14) can always converge to a near-optimal solution for the BA problem [1](9).*

Consider the following function

$$h_{\mathbf{V}}(\mathbf{x}) := \left\| \frac{\mathbf{x}}{\|\mathbf{x}\|} - \mathbf{V} \right\|^2, \tag{9}$$

where  $\mathbf{x} \in \mathbb{R}^3$ ,  $\mathbf{V} \in \mathbb{R}^3$  ( $\|\mathbf{V}\| = 1$ ). It is a fact that

$$h_{\mathbf{V}}(\mathbf{x} + \lambda \Delta \mathbf{x}) \leq \max\{h_{\mathbf{V}}(\mathbf{x}), h_{\mathbf{V}}(\mathbf{x} + \Delta \mathbf{x})\} \tag{10}$$

for any  $\Delta \mathbf{x} \in \mathbb{R}^3$  and any  $\lambda \in (0, 1)$ .

Considering the NLS problem [1](14) and the linearity of  $\bar{\mathbf{N}}_{j,i}$  w.r.t.  $\mathbf{p}$ , the objective of [1](14) can be rewritten as

$$\begin{aligned} \min_{\{\mathbf{p}\}} h(\mathbf{p}, \bar{\mathbf{R}}, \bar{\mathbf{F}}) &= \min_{\{\mathbf{p}\}} \sum_{i \in \mathbb{T}_j, j} \left\| \frac{\bar{\mathbf{A}}_i \mathbf{p}}{\|\bar{\mathbf{A}}_i \mathbf{p}\|} - \bar{\mathbf{V}}_{ij} \right\|^2 \\ &= \min_{\{\mathbf{p}\}} \sum_{i \in \mathbb{T}_j, j} h_{\mathbf{v}_i}(\bar{\mathbf{A}}_i \mathbf{p}), \end{aligned} \quad (11)$$

where  $\bar{\mathbf{V}}_{ij} := \bar{\mathbf{R}}_i \mathbf{v}_{ij}^{(l)}$  is a directional vector.

From (10), we come to an important observation concerning convergence:

For any  $\Delta \mathbf{p} \in \mathbb{R}^{3M}$  and  $\lambda \in (0, 1)$ ,

$$\begin{aligned} h(\mathbf{p} + \lambda \Delta \mathbf{p}, \bar{\mathbf{R}}, \bar{\mathbf{F}}) &= \sum_{i \in \mathbb{T}_j, j} h_{\mathbf{v}_i}(\bar{\mathbf{A}}_i(\mathbf{p} + \lambda \Delta \mathbf{p})) \\ (\text{using (10)}) &\leq \sum_{i \in \mathbb{T}_j, j} \max\{h_{\mathbf{v}_i}(\bar{\mathbf{A}}_i \mathbf{p}), h_{\mathbf{v}_i}(\bar{\mathbf{A}}_i(\mathbf{p} + \Delta \mathbf{p}))\} \\ &\leq h(\mathbf{p}, \bar{\mathbf{R}}, \bar{\mathbf{F}}) + h(\mathbf{p} + \Delta \mathbf{p}, \bar{\mathbf{R}}, \bar{\mathbf{F}}) \end{aligned} \quad (12)$$

Denoting the optimal solution of the NLS problem in [1](14) as  $\bar{\mathbf{p}}$ , i.e.,  $h(\bar{\mathbf{p}}, \bar{\mathbf{R}}, \bar{\mathbf{F}}) = 0$ , we have

$$h(\bar{\mathbf{p}} + \lambda \Delta \mathbf{p}, \bar{\mathbf{R}}, \bar{\mathbf{F}}) \leq h(\bar{\mathbf{p}} + \Delta \mathbf{p}, \bar{\mathbf{R}}, \bar{\mathbf{F}}) \quad (13)$$

The inequality indicates the fact that function  $h$  is non-decreasing in each direction of  $\Delta \mathbf{p}$  starting from  $\bar{\mathbf{p}}$  to  $\bar{\mathbf{p}} + \Delta \mathbf{p}$ . With any initial guess  $\mathbf{p} \in \mathbb{R}^{3M}$ , convergence to its optimal point is guaranteed with successive applications of steepest descent.

Under noise-free conditions,  $\bar{\mathbf{R}}$  is same as the global minimum,  $h(\bar{\mathbf{p}}, \bar{\mathbf{R}}, \bar{\mathbf{F}})$  is now also the global minimum of the original PMBA objective [1](9). Under low-noise conditions,  $\bar{\mathbf{R}}$  is close to the optimal estimate,  $\bar{\mathbf{p}}$  is also a near-optimal solution of the original PMBA [1](9). This idea has also been discussed in [3].

### 3 More supporting data

We show PMBA test results on our own datasets. Images for the Usyd-mainquad and Victoria-cottage are taken at Sydney University campus using our self-developed portable mapping platform. The fake-pile images are taken from the Google Tango device [2]. All datasets can be downloaded from OpenSLAM<sup>1</sup>.

---

<sup>1</sup> <https://svn.openslam.org/data/svn/ParallaxBA/>

### 3 .1 PMBA convergence results

In this section we present more convergence plots illustrating the efficiency and accuracy of our PMBA formulation. See Figure 1. The plots show Mean Square Error (labeled as Chi<sup>2</sup>) at each stage of iteration. As explained in [1], although PMBA uses a ray direction based cost function. For fairness of comparison, we compute its corresponding UV pixel error. Despite this treatment, PMBA is able to reach good global minimum better than or close to the best results other BA's can achieve.

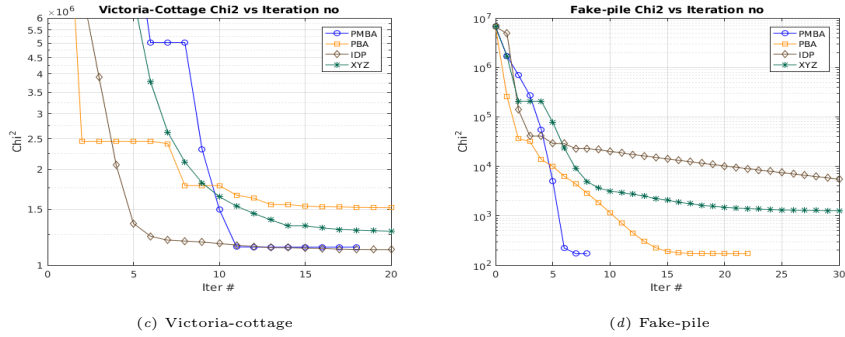


Fig. 1: Convergence plots for PMBA, PBA, IDP and XYZ

### 3 .2 Reconstruction results from PMBA

We present reconstruction results from our collected outdoor data sets. See Fig 2 and 3.

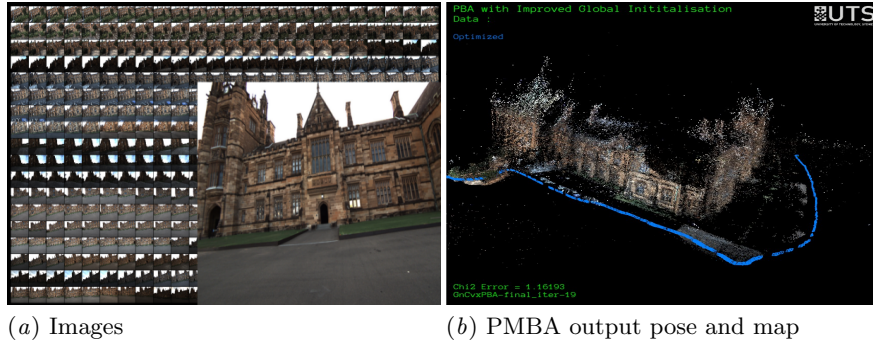


Fig. 2: Usyd-mainquad dataset

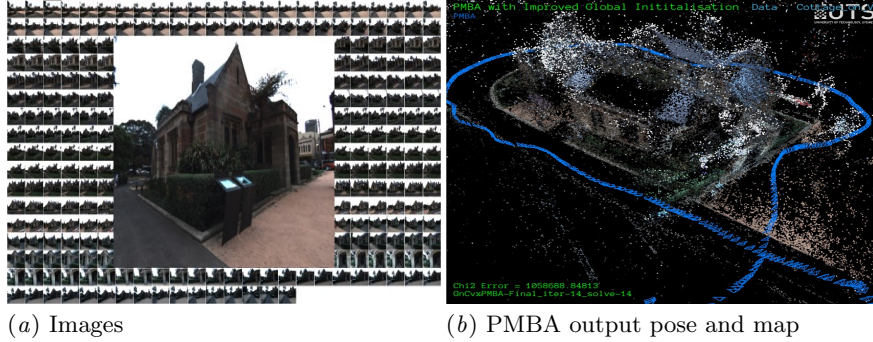


Fig. 3: Victoria-cottage dataset

### 3 .3 Results of full PMBA pipeline at various stages

We use publicly available datasets to test our full PMBA pipeline. We use Ladybug-1370, Trafalgar-126 and Venice-427 datasets from “Bundle adjustment in the large” (BAL) database<sup>2</sup>, and the College dataset from OpenSLAM. We present screenshots at various stages of our pipeline in Fig. 4, 5, 6, and 7. In the snapshots, the PMBA pipeline data is in blue, reference data is in red. BAL is the reference data in tests that take BAL inputs. PBA generated results is the reference data in the College dataset. In all figures, column 1 shows optimization results at CLS stage, column 2 shows selected iteration results in NLS initialization, column 3 is a typical iteration result in full-PMBA stage and column 4 shows the final map.

The figures shows that reasonable initial values were formed at CLS stage. The NLS pose-graph stage has a very large convergence region such that imperfect outputs from the CLS stage can gradually converge to motion trajectory with a topology similar to that of Ground Truth. This is especially obvious in “Ladybug-1370” and “Venice-427”. We notice that in “Ladybug-1370”, BAL’s optimal trajectory (in red) contains an erroneous camera pose, shown as red dot at top right corner of the red trajectory, our method did not encounter this stray pose at all.



Fig. 4: Ladybug-1370 results

<sup>2</sup> <http://grail.cs.washington.edu/projects/bal/>

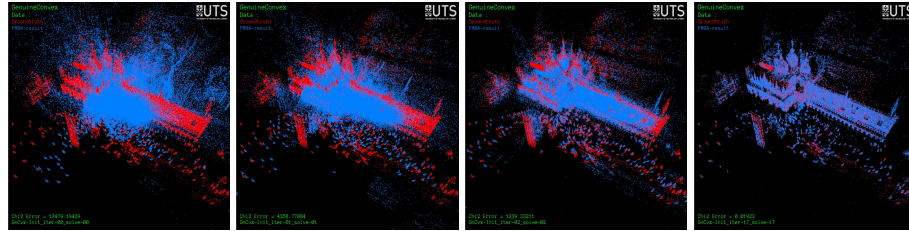


Fig. 5: Venice-427 results

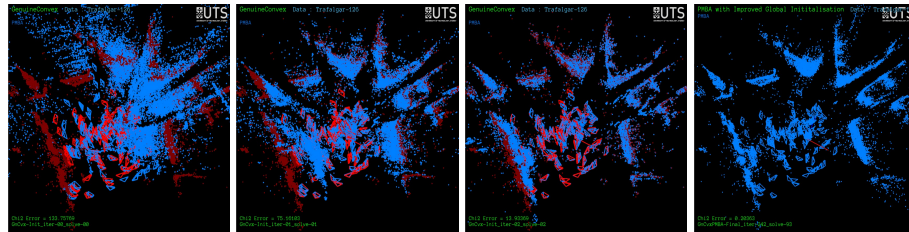


Fig. 6: Trafalgar-126

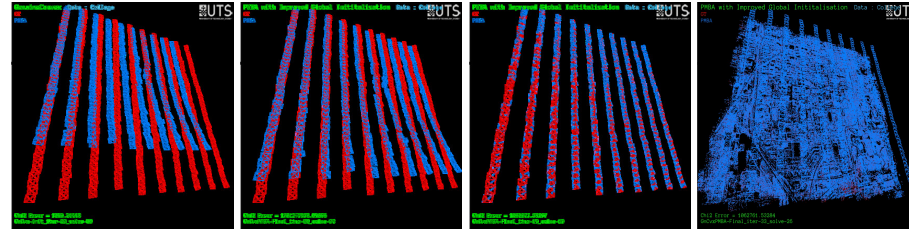


Fig. 7: Ladybug-1370 results

## A Appendix – Global ray re-examined

For ease of mathematical manipulation, define

$$\mathbf{a} = \mathbf{p}_{m_j} - \mathbf{p}_{a_j}, \quad \mathbf{b} = \mathbf{p}_{m_j} - \mathbf{p}_i, \quad \mathbf{n}_m = \mathbf{R}_{m_j} \mathbf{n}_{m_j} \quad (14)$$

From Figure [1] 2, we can see that  $\alpha_j$  is the angle between  $\mathbf{a}$  and  $\mathbf{n}_m$ , so compute its sine and cosine as

$$\sin(\alpha_j) = \frac{\|\mathbf{a} \times \mathbf{n}_m\|}{\|\mathbf{a}\| \|\mathbf{n}_m\|} = \frac{\|\mathbf{a} \times \mathbf{n}_m\|}{\|\mathbf{a}\|}, \quad \cos(\alpha_j) = \frac{\mathbf{a} \cdot \mathbf{n}_m}{\|\mathbf{a}\| \|\mathbf{n}_m\|} = \frac{\mathbf{a}^\top \mathbf{n}_m}{\|\mathbf{a}\|}$$

For easy of subsequent Jacobian derivation. we re-write the expression of observation ray vector from [1](7) as

$$\begin{aligned} \mathbf{N}_{j,i} &= \sin(\alpha_j - \theta_j) \|\mathbf{p}_{m_j} - \mathbf{p}_{a_j}\| \mathbf{R}_{m_j} \mathbf{n}_j + \sin(\theta_j) (\mathbf{p}_{m_j} - \mathbf{p}_i) \\ &= \sin(\alpha_j - \theta_j) \|\mathbf{a}\| \mathbf{n}_m + \sin(\theta_j) \mathbf{b} \\ &= \cos(\theta_j) \frac{\|\mathbf{a} \times \mathbf{n}_m\|}{\|\mathbf{a}\|} \|\mathbf{a}\| \mathbf{n}_m - \sin(\theta_j) \frac{\mathbf{a}^\top \mathbf{n}_m}{\|\mathbf{a}\|} \|\mathbf{a}\| \mathbf{n}_m + \sin(\theta_j) \mathbf{b} \\ &= \cos(\theta_j) \|\mathbf{a} \times \mathbf{n}_m\| \mathbf{n}_m - \sin(\theta_j) (\mathbf{b} - (\mathbf{a}^\top \mathbf{n}_m) \mathbf{n}_m) \end{aligned} \quad (15)$$

## B Appendix – Jacobians

From [1](9), an observation's jacobian can be calculated as

$$\frac{\partial \mathbf{e}_{i,j}}{\partial \mathcal{X}_{j,i}} = \frac{\partial \check{\mathbf{N}}_{j,i}}{\mathcal{X}_{j,i}} \quad (16)$$

### B .1 Jacobian of observation ray

The global ray direction in [1](9)  $\check{\mathbf{N}}_{j,i}$  can be computed as

$$\check{\mathbf{N}}_{j,i} = \xi(\mathbf{N}), \quad \xi(\mathbf{x}) = \frac{\mathbf{x}}{\|\mathbf{x}\|} \quad (17)$$

where  $\xi$  is the normalization function. And its derivative is

$$\partial \xi(\mathbf{x}) = \frac{1}{\|\mathbf{x}\|} \mathbf{I}_3 - \frac{1}{\|\mathbf{x}\|^3} \mathbf{x} \mathbf{x}^\top \quad (18)$$

Therefore (16) becomes

$$\frac{\partial \mathbf{e}_{i,j}}{\partial \mathcal{X}_{j,i}} = \partial \xi(\mathbf{N}_{j,i}) \frac{\partial \mathbf{N}_{j,i}}{\mathcal{X}_{j,i}} \quad (19)$$

Define Jacobians of ray  $\mathbf{N}$  with respect to  $\mathbf{n}_m$ ,  $\mathbf{a}$ ,  $\mathbf{b}$  and parallax angle  $\theta_j$  as

$$\begin{aligned} \mathbf{J}_{n_m}^N &= \frac{\partial \mathbf{N}}{\partial \mathbf{n}_m} = \cos(\theta_j)(\|S(\mathbf{a})\mathbf{n}_m\| \mathbf{I}_3 + \mathbf{n}_m \frac{(S(\mathbf{a})\mathbf{n}_m)^\top}{\|S(\mathbf{a})\mathbf{n}_m\|} S(\mathbf{a})) - \sin(\theta_j)(\mathbf{n}_m \mathbf{a}^\top + (\mathbf{a}^\top \mathbf{n}_m) \mathbf{I}_3) \\ \mathbf{J}_a^N &= \frac{\partial \mathbf{N}}{\partial \mathbf{a}} = -\cos(\theta) \mathbf{n}_m \frac{(S(\mathbf{a})\mathbf{n}_m)^\top}{\|S(\mathbf{a})\mathbf{n}_m\|} S(\mathbf{n}_m) - \sin(\theta_j) \mathbf{n}_m \mathbf{n}_m^\top \\ \mathbf{J}_b^N &= \frac{\partial \mathbf{N}}{\partial \mathbf{b}} = \sin \theta_j \\ \mathbf{J}_\theta^N &= \frac{\partial \mathbf{N}}{\partial \theta_j} = -\sin(\theta) \|\mathbf{a} \times \mathbf{n}_m\| \mathbf{n}_m + \cos(\theta_j) (\mathbf{b} - (\mathbf{a}^\top \mathbf{n}_m) \mathbf{n}_m) \end{aligned} \quad (20)$$

The Jacobian of  $\mathbf{N}$  w.r.t. the main anchor is

$$\partial_m \mathbf{N} = \mathbf{J}_{n_m}^N \partial_m \mathbf{n}_m + \mathbf{J}_a^N \partial_m \mathbf{a} + \sin(\theta_j) \partial_m \mathbf{a} \quad (21)$$

The Jacobian of  $\mathbf{N}$  w.r.t. the associated anchor is

$$\partial_a \mathbf{N} = \mathbf{J}_a^N \partial_a \mathbf{a} \quad (22)$$

The Jacobian of  $\mathbf{N}$  w.r.t. the current pose is

$$\partial_i \mathbf{N} = -\sin(\theta_j) \mathbf{I}_3 \quad (23)$$

The Jacobian of  $\mathbf{N}$  w.r.t. the feature is

$$\partial_f \mathbf{N} = \mathbf{J}_{n_m}^N (\partial_f \mathbf{n}_m) + \mathbf{J}_\theta^N \quad (24)$$

The Jacobians of  $\mathbf{n}_m$

$$\begin{aligned}\partial_m \mathbf{n}_m &= [-\mathbf{R}_{m_j} S(\mathbf{n}_j) \quad \mathbf{0}_{3,3}], \\ \partial_f \mathbf{n}_m &= [-\mathbf{R}_{m_j} S(\mathbf{n}_j) \mathbf{C}],\end{aligned}\tag{25}$$

The Jacobians of  $\mathbf{a}$

$$\begin{aligned}\partial_m \mathbf{a} &= [\mathbf{0}_{3,3} \quad \mathbf{R}_m] \\ \partial_a \mathbf{a} &= [\mathbf{0}_{3,3} \quad -\mathbf{R}_a]\end{aligned}\tag{26}$$

## B .2 Jacobians of observations to state variables

The jacobian for an observation (factor) with respect to each involved state variable (vertex) is given in Table 1.

Table 1: Jacobian for a factor node

Involved vertices	Jacobian calculation
Main anchor	$\partial \xi \partial_m \mathbf{N}$
Associated Achor	$\partial \xi \partial_a \mathbf{N}$
Jacobian For Pose $i$	$\partial \xi \partial_i \mathbf{N}$
Jacobian For feature $(\mathbf{n}, \theta)$	$\partial \xi \partial_f \mathbf{N}$

## B .3 Special factor $m_j$ : current pose is main anchor

**Involved vertexes** : Obviously, this factor only involves one vertex – feature  $(\mathbf{n}, \theta)$ .

### Error function

$$\begin{aligned}\mathbf{e}_{i,j} &= \xi(\mathbf{N}_{m_j,j}) - \mathbf{z}, \quad \mathbf{N}_{m_j,j} = \mathbf{R}_{m_j} \mathbf{n}, \quad \|\mathbf{N}_{m_j,j}\| = 1 \\ \partial \xi(\mathbf{N}_{m_j,i}) &= 1\end{aligned}\tag{27}$$

### Jacobian For $(\mathbf{n}, \theta)$

$$[0 \quad S(\mathbf{n}) \mathbf{A}_n]\tag{28}$$

where  $n$  is the feature's local direction vector and  $\mathbf{A}_n$  is its the null space.

#### B .4 Special factor $a_j$ : current pose is associate anchor

This factor involves three vertices:  $\mathbf{X}_m$ ,  $\mathbf{X}_a$  and  $(\mathbf{n}, \theta)$ .

Since  $\mathbf{p}_{a_j}$  and  $\mathbf{p}_i$  are the same positions, we have  $\mathbf{a} = \mathbf{b}$ , so the Jacobians for ray  $\mathbf{N}_{j,a_j}$  can be simplified as:

$$\begin{aligned}\mathbf{N}_{j,a_j} &= \cos(\theta_j) \|\mathbf{a} \times \mathbf{n}_m\| \mathbf{n}_m + \sin(\theta_j) (\mathbf{a} - (\mathbf{a}^\top \mathbf{n}_m) \mathbf{n}_m) \\ \mathbf{J}_{\theta_j}^N &= -\sin(\theta) \|\mathbf{a} \times \mathbf{n}_m\| \mathbf{n}_m + \cos(\theta_j) (\mathbf{a} - (\mathbf{a}^\top \mathbf{n}_m) \mathbf{n}_m) \\ \mathbf{J}_a^N &= -\cos(\theta_j) \mathbf{n}_m \frac{(S(\mathbf{a}) \mathbf{n}_m)^\top}{\|S(\mathbf{a}) \mathbf{n}_m\|} S(\mathbf{n}_m) - \sin(\theta_j) \mathbf{n}_m \mathbf{n}_m^\top + \sin(\theta_j) \mathbf{I}_3\end{aligned}\tag{29}$$

Note that  $\mathbf{J}_{n_m}^N$  is same as (20).

## References

1. L. Liu, T. Zhang, Y. Liu, B. Leighton, L. Zhao, Huang, S., Dissanayake, G.: Parallax bundle adjustment on manifold with improved global initialization. In: WAFR 2018
2. Liu, L., Wang, Y., Zhao, L., Huang, S.: Evaluation of Different SLAM Algorithms using Google Tangle Data. In: 2017 IEEE Conference on Industrial Electronics and Applications. 10.1109/ICIEA.2017.8283158
3. Wilson, K., Snavely, N.: Robust Global Translations with 1DSfM. In: Proceedings of the European Conference on Computer Vision (ECCV) 2014. doi: 10.1007/978-3-319-10578-9\_5